Materials Research. 2017; 20(1): 256-263
DOI: http://dx.doi.org/10.1590/1980-5373-MR-2016-0292

Effect of Capping Agent on the Morphology, Size and Optical Properties of In_2O_3 Nanoparticles

Ch. Kanchana Latha[a], Mucherla Raghasudha[b]*, Y. Aparna[a], Ramchander. M[c], D. Ravinder[d], Jaipal. K[e], P. Veerasomaiah[b], D. Shridhar[f]

[a] *Department of Physics, Jawaharlal Nehru Technological University Hyderabad – JNTUH, College of Engineering Hyderabad – CEH, Hyderabad, Telangana, India*
[b] *Department of Chemistry, University College of Science, Osmania University, Hyderabad, Telangana, India*
[c] *Department of Bio Chemistry, Mahatma Gandhi University, Nalgonda, Telangana, India*
[d] *Department of Physics, Osmania University, Hyderabad, Telangana, India*
[e] *Inorganic & Physical Chemistry Division, Indian Institute of Chemical Technology – IICT, Hyderabad, Telangana, India*
[f] *Department of Physics, Khairatabad Government Degree College, Hyderabad, Telangana, India*

Received: April 10, 2016; Revised: October 17, 2016; Accepted: November 21, 2016

The Indium Oxide (In_2O_3) nanoparticles were synthesized through Acacia gum mediated method with the surfactants CTAB (Cetyl Trimethyl Ammonium Bromide) and SDBS (Sodium Docecyl Benzene Sulfonate). The characterization of the synthesized In_2O_3 nanoparticles was carried out by XRD, FTIR, RAMAN, TEM, SEM, EDAX, UV-Vis and PL techniques. TG-DTA analysis was performed to know the calcination temperature of In_2O_3 nanoparticles. XRD analysis confirmed the crystalline nature of the synthesized In_2O_3 nanoparticles. The morphology and chemical composition were characterized by TEM, SEM and EDAX respectively. It was observed that morphology and size of synthesized nanoparticles measured by TEM and SEM analysis were dependent on the type of capping agent (surfactant) used. Raman and UV-Vis spectral analysis confirmed that the band gap value of CTAB capped In_2O_3 particles were larger than the SDBS capped In_2O_3 particles. FTIR analysis indicated that the bands were stretched in In_2O_3 particles capped by SDBS than by CTAB. From the photoluminescence studies (PL technique), a blue shift in the emission peaks of CTAB and SDBS capped In_2O_3 particles was observed that indicates larger optical band gap than the bulk.

Keywords: *Indium Oxide nanoparticles, CTAB and SDBS capping agents, Raman Spectra, Visible spectra, PL technique*

1. Introduction

Indium Oxide (In_2O_3) is an important *n*-type semiconductor. It has a wide band gap of approximately 3.6eV, shows high transparency in the visible region and excellent electrical conductivity[1]. Semiconductor nanomaterials with a wide band gap have potential applications in nonlinear optics and optoelectronics[2]. It has fascinating properties such as strong interaction between certain poisonous gas molecules and its surfaces[3]. These properties make In_2O_3, a remarkable material for a variety of applications such as solar cells[4], Liquid Crystal Displays[5], Architectural Glasses[6], Gas Sensors[7], Flat Panel Display[8], and in Photo-catalytic conversions[9]. To widen the technological applications of In_2O_3, investigations were made to synthesize them in different forms such as nanotubes, nanobelts, nano wires and nanoparticles. The properties of nanomaterials not only depend on the composition of the material but also depend on its size and shape which are influenced by the method of synthesis.

In_2O_3 nanoparticles have been synthesized by several methods such as sol–gel method[10], pulse laser deposition[11], thermal decomposition[12], thermal hydrolysis[13], micro-emulsion method[14], spray pyrolysis[15], mechanical chemical processing method[16], hybrid induction and laser heating (HILH) method[17], non-aqueous synthesis[18], and hydrothermal synthesis[19]. Among various synthesis methods, simple and cost effective route that use cheap, non-toxic and eco-friendly materials is the area of interest. One such simple method is gum mediated technique. Besides this, surfactants play an essential role in controlling morphology of nanostructure. It is because of their soft - template effect, ability to modify the chemical kinetics and simple maneuverability.

In the present work, In_2O_3 nanocrystals with size 16-17nm have been successfully synthesized through simpler and easiest gum mediated method using CTAB (Cetyl Trimethyl Ammonium Bromide) and SDBS (Sodium Docecyl Benzene Sulfonate) as capping agents. It is reported that capping assisted synthesis yielded very fine nanoparticles than non-capping mediated routes[20].

* e-mail: raghasudha_m@yahoo.co.in

2. Materials and methods

Indium III Acetylacetonate (99.99% purity, Sigma Aldrich), Acacia gum (from Dawaa Saas in local market of Hyderabad), CTAB (Sigma Aldrich) and SDBS (Sigma Aldrich) were used as starting materials as purchased without further purification for the synthesis of In_2O_3 nanoparticles.

1g of Indium III Acetylacetonate, 0.25g of Acacia gum and 0.25g of CTAB are mixed thoroughly by using mortar and pestle for the synthesis of CTAB capped In_2O_3 nanoparticles. In a similar manner SDBS capped In_2O_3 nanoparticles were synthesized by mixing 1g of Indium III Acetylacetonate , 0.25g of SDBS and 0.25g of Acacia gum in mortar and pestle.

Prepared Indium oxide particles capped by the two surfactants were subjected to TG-DTA analysis (Thermo gravimetric-differential thermal analysis) to know the calcination temperature. X-ray diffraction patterns were recorded using X-ray diffractometer with Cuk_α (λ=1.5406 A^o) in the range of 20-80^o (2θ) to know the crystal phase. An energy-dispersive X-ray Spectrometer (EDX) equipped with the Scanning Electron Microscopy was used to determine the morphology and sample composition. Transmission Electron Microscope (TEM), High Resolution Transmission Electron Microscope (HRTEM) and Selected Area Electron Diffraction (SAED) on a JEOLJEM microscope operated at 200kV were used to know the surface morphology and crystallite size. FTIR spectra, Raman spectra, UV-vis absorption spectrum and the Photo Luminescence spectrum were recorded to know the band gap in the prepared nanoparticles capped by different capping agents.

3. Results and Discussion

3.1. TG-DTA Analysis (Thermo gravimetric-Differential Thermal Analysis)

There is an endothermic peak at 191.9^{o}C for CTAB and 190^{o}C for SDBS corresponding to the evaporation of OH as shown in Figure 1. The endothermic peak at 279^{o}C for CTAB and 269.4^{0}C for SDBS indicates the heat released by decomposition of organic substance in CTAB and SDBS. This is due to the existence of organic solvent, CO and OH desorption. A small exothermic peak at 720^{o}C for CTAB and 730^{o}C for SDBS was observed. At these temperatures, CTAB and SDBS are considered to enter into In_2O_3 crystal lattice respectively. The final mass loss in the TGA group was 4% and 6% for CTAB and SDBS respectively. The calcination temperature can be taken as 730^{o}C for the prepared In_2O_3 particles. Hence, nano sized yellow powder of In_2O_3 is obtained by calcining the prepared material at 730^{o}C for both CTAB & SDBS surfactants for 2 hours in air.

3.2. XRD Analysis

The XRD patterns of In_2O_3 nanoparticles capped with CTAB and SDBS were shown in Figure 2. The major diffraction peaks (2 2 2), (4 0 0), (4 4 0) and (6 6 2) observed in the figure are indexed to the cubic bixbyite structure of In_2O_3 as evidenced from JCPDS No.06-0416.

There is no impurity peak found indicating the formation of pure sample. The XRD peaks of In_2O_3 were sharp in case of SDBS capping than that of CTAB capping which indicates good crystallinity of nanoparticles. The average crystallite size of the prepared In_2O_3 nanoparticles capped by CTAB and SDBS was calculated by using Scherrer's equation[21] and was estimated as 16.6 nm and 17.4 nm respectively. The lattice parameters calculated using maximum intensity peak (222) plane were found to be 10.095Å for CTAB and 10.023Å for SDBS capped In_2O_3 nanoparticles respectively. The values were reported in Table 1 and were found to be in good agreement with the literature[22].

3.3. EDAX and SEM Analysis

The surface morphology of the respective CTAB and SDBS capped In_2O_3 nanoparticles were analysed using SEM, and the images are presented in Figure 3. The images show that the CTAB capped In_2O_3 NPs were spherical in shape and SDBS capped In_2O_3 NPs were like spherical clusters with porous structure. The morphology of In_2O_3 nanoparticles prepared in the present study show a well patterned distribution of nanocrystalline grains with porous nature. This spherical and porous nature renders them suitable for gas sensing applications. EDAX patterns of prepared In_2O_3 nanoparticles stabilized by Acacia gum extract obtained from CTAB and SDBS capping agents are shown in Figure 3.

Strong signals from *In* and *O* atoms are recorded. From the EDAX data (table 2), it is clear that there is no reference to other phases. This confirms that the CTAB and SDBS capped In_2O_3 samples contains pure *In* and *O* phases as evident from Table 2.

There is loss in atomic % of In in CTAB. It may be due to the presence of traces of (Na, S and Br) which might have occurred in the process of calcination. The atomic ratio of *In* and *O* was found to be 2:3 which is nearer to the stoichiometry ratio of In_2O_3. The discrepancy in the stoichiometry may be due to the presence of oxygen vacancies. These vacancies may be created during the calcination in the static atmosphere i.e. box-type muffle furnace.

3.4. TEM , HRTEM & SAED

The morphology and the structure of the In_2O_3 nanoparticles were investigated by TEM. From the TEM images shown

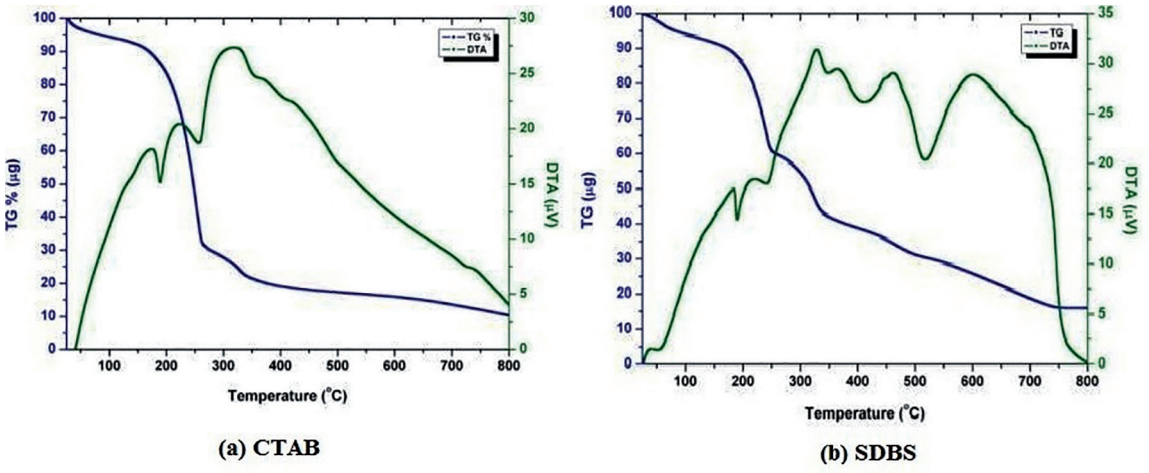

Figure 1: TG-DTA curves of thermal decompostion of In_2O_3 capped with (a) CTAB (b) SDBS at a heating rate of 10oC/min in static air

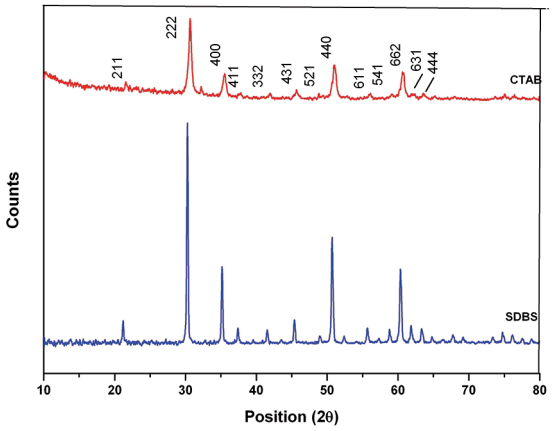

Figure 2: XRD Pattern of In_2O_3 samples capped with (a) CTAB (b) SDBS calcined at 650°C in air for 2 hours

in Figure 4, it was found that the In_2O_3 particles capped by CTAB were like spherical balls and that capped by SDBS were like spherical clusters. Their average sizes were found to be 15-20nm capped by CTAB and 20-25nm capped by SDBS respectively which are in good agreement with those values calculated by XRD analysis. The corresponding selected-area electron diffraction (SAED) patterns (Figure 4) of CTAB and SDBS capped In_2O_3 samples show spotty ring patterns without any additional diffraction spots and rings of second phases, revealing their crystalline cubic structure. The interplanar spacing d_{hkl} from SAED patterns for CTAB and SDBS capped In_2O_3 nanoparticles was in good agreement with the values in the standard data (JCPDS: 06-0416) as summarized in Table 3. The high-resolution TEM images confirm that the synthesized particles are crystalline in nature. The nanoparticles are clearly well identified and no effective aggregation of bulk particles is observed. This fact indicates the effective capping of CTAB and SDBS on the surface of nanoparticles.

3.5. Raman Spectra Analysis

The acquired Raman spectra of CTAB and SDBS capped In_2O_3 nanoparticles also provides the evidence for the cubic In_2O_3 nanoparticles . The observed Raman peaks from the figure 5 at 160, 304, 626, 989 cm^{-1} for CTAB capped and 213, 404, 600, 1371 cm^{-1} for SDBS capped In_2O_3 Nanoparticles are ascribed to the phonon vibration modes of cubic In_2O_3 nanoparticles. The values are in good agreement with those reported in the literature[23,24]. Raman spectra related to the pure vibrational modes and the peaks at 160 cm^{-1} for CTAB and 213cm^{-1} for SDBS capping agrees with the reported value in literature[25,26]. It is found that the vibrational modes of SDBS capped are finer than that of CTAB capped In_2O_3 nanoparticles.

3.6. UV and Tauc's Plot

The UV-Vis absoption spectra of the as-prepared In_2O_3 nanoparticles dispersed in Ethylene Glycol are shown in Figure 6(a). The prepared nanoparticles with the capping agents CTAB showed a band edge at 288nm whereas those prepared with the capping of SDBS showed the band at 292nm. This fact is due to the excitonic transition of the valence

Table 1: Average Particle size and Cubic Lattice parameter of In_2O_3 samples capped with CTAB and SDBS from XRD, TEM analysis

In_2O_3 nanoparticles prepared from	Average lattice parameter '*a*' in A^0 for (222) plane	Average size (nm) from XRD	Average size (*nm*) from TEM
CTAB capping	10.095	16.6	15-20
SDBS capping	10.023	17.4	20-25

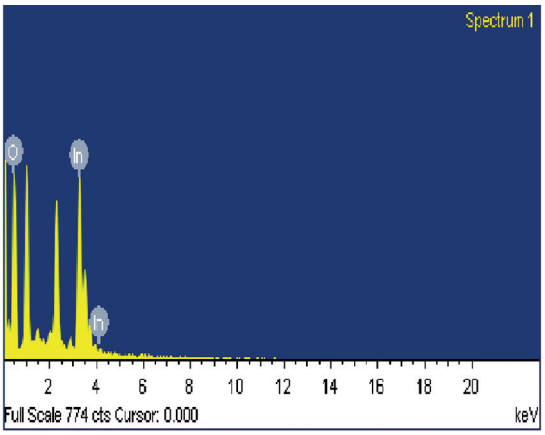

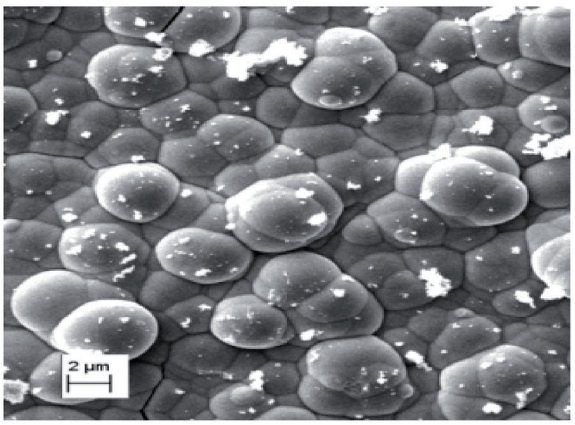

Fig. 3(a)

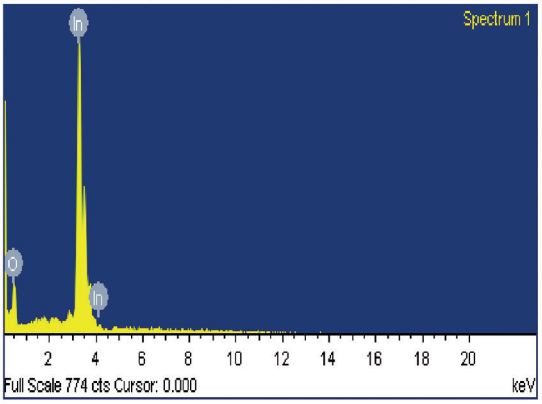

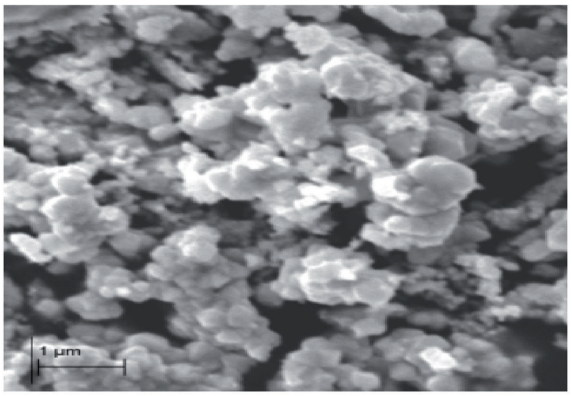

Fig. 3(b)

Figure 3: EDAX and SEM images of In_2O_3 samples capped with (a) CTAB (b) SDBS

Table 2: EDAX data of In_2O_3 samples capped with CTAB and SDBS

	(CTAB) capping		(SDBS) capping	
	In	O	*In*	O
Atomic %	22.86	77.14	23.25	76.75
Weight %	46.67	71.33	17.35	22.65

Table 3: Interplanar Spacings of In_2O_3 samples capped with CTAB and SDBS from SAED patterns of Fig.4 with standard JCPDS(06-0416)data

	In_2O_3 capped with		Standard JCPDS:06-0416	
Ring No.	CTAB	SDBS		
	d_{hkl}	d_{hkl}	d_{hkl}	*h k l*
R1	1.011	-	1.0414	511
R2	1.619	-	1.5622	222
R3	2.718	2.635	2.7056	200
R4	1.935	2.205	1.9134	220
R5	0.99	-	0.9566	440
R6	1.322	1.395	1.353	400
R7	-	1.124	1.1047	422
R8	-	1.71	1.6318	311

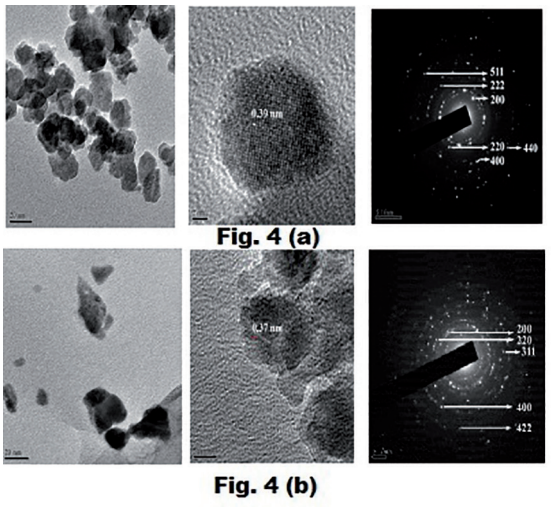

Figure 4: TEM, HRTEM and SAED (Selected Area Electron Diffraction) patterns of In_2O_3 samples capped with (a) CTAB (b) SDBS

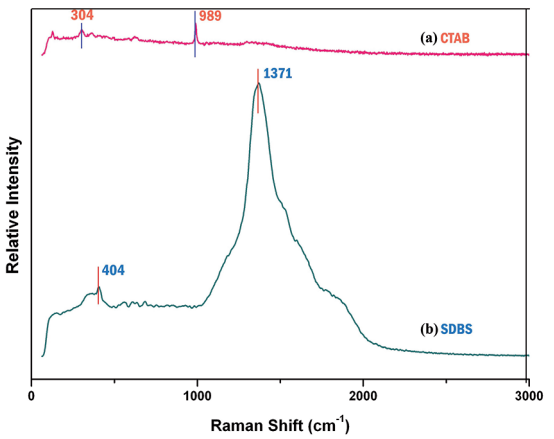

Figure 5: Raman Spectra of In_2O_3 samples capped with CTAB and SDBS

band electrons to the conduction band[27]. The blueshift in the absopntion edge of the nanoparticles prepared by using the surfactants CTAB and SDBS reveals their low partcile size.

Figure 6(b) and fig.6(c) represents the Tauc's plot for In_2O_3 nanoparticles obtained from optical absoption data by plotting $(\alpha hv)^2$ vs hv (photo energy) where, α, h and v are the absorption coefficient, Planck's constant and photo frequency respectively. The inflections of the plots afforded band gap values of 3.844eV for CTAB and 3.857eV for SDBS capped In_2O_3 nanoparticles respectively. These values are higher than the bulk band gap values of In_2O_3. The band gap value of CTAB capped In_2O_3 is larger than the SDBS capped In_2O_3 nanoparticles. Hence, the stronger ionic interaction of CTAB than that of SDBS with In_2O_3 has resulted in smaller size nanoparticles.

3.7. FTIR Analysis

The bands around 2925cm^{-1}, 2858cm^{-1} and 1416cm^{-1} can be ascribed to the C-H vibration of the organics. The band at 1050cm^{-1} is attributed to the absorption of C-O vibration, while the absorptions around 500 cm^{-1} are due to *In-O* vibrations[28]. The peak at 1568cm^{-1} appeared on the IR spectrum is due to C-O vibrations from the Acetylacetone species[29]. Based on the experiments, it can be reported that the acetylacetone species coordinated to In^{3+} cations on the particle surface could be substituted by the capping agents during the biosynthesis process.The bands of CTAB & SDBS Capped In_2O_3 nanoparticles are in good agreement with the literature values and are stretched in SDBS than in CTAB capped as shown in Figure 7 & Table 4.

3.8. PL Analysis

Photo Luminescence emission was mainly attributed to the presence of vacancies or defects. Vacancies may be Indium or Oxygen vacancies, while the defects may be interestial Indium or anti-site Oxygen[30]. Vacancies present in the materials induce the formation of new energy levels in the bandgap and as a result emissions will arise from their trap levels. While exciting the sample, emissions occur due to radiative recombination of a photo excited hole with an electron and the emission peaks are commonly referred to as deep level or trap state emissions due to oxygen vacancies[31]. The luminescent property of the prepared In_2O_3 cubic crystal capped by CTAB and STBS, calcined at 650 ^{0}C was analyzed by exciting the sample at 310nm wavelength of Xenon lamp. Figure 8 shows the room temperature Photo Luminescence (PL) Spectra of In_2O_3 samples capped with CTAB and SDBS. The spectra of CTAB capped In_2O_3 NPs exhibited a strong emission with its maximum at 342nm and a few broad peaks centered at 400nm and 425nm. Whereas, in the PL spectra of SDBS capped In_2O_3 NPs, the maximum was observed at 326nm and a very few broad peaks were centered at 400nm and 430nm.The maximum absorption observed at 326nm and 342nm may be accounted for by deep-level emissions due to amorphous In_2O_3, and very few broad peaks at around 400nm to 425nm may be due to Indium interstitials and Oxygen vacancies (Impurities)[32]. A blue shift observed in the emission peaks of CTAB and SDBS capped In_2O_3 nanoparticles indicates the presence of In_2O_3 NPs only.

4. Conclusion

The In_2O_3 nanoparticles were prepared using two capping agents (CTAB and SDBS). They exhibited different particle size and morphology, which were studied from XRD,

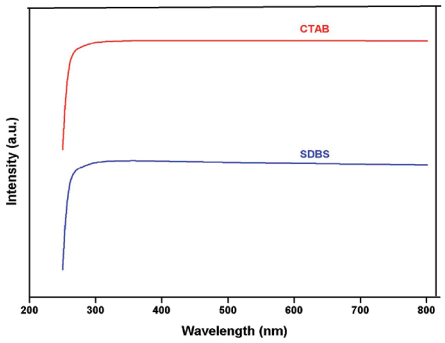

Fig. 6 (a)

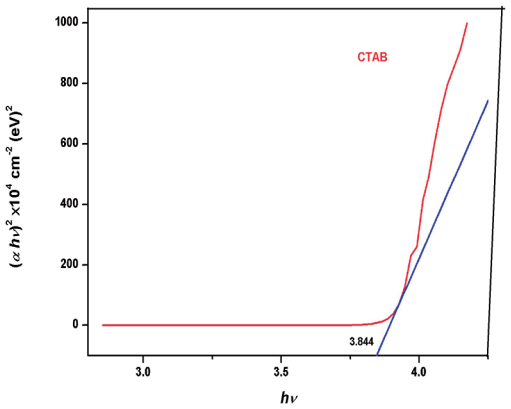

Fig. 6 (b)

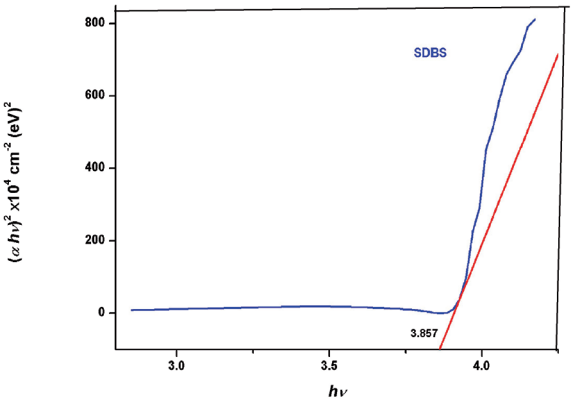

Fig. 6 (c)

Figure 6: Room temperature Optical Absorbance Spectra of In_2O_3 samples capped with (a) UV-Vis absoption spectra of In_2O_3 samples capped with CTAB and SDBS and (b) CTAB and (c) SDBS

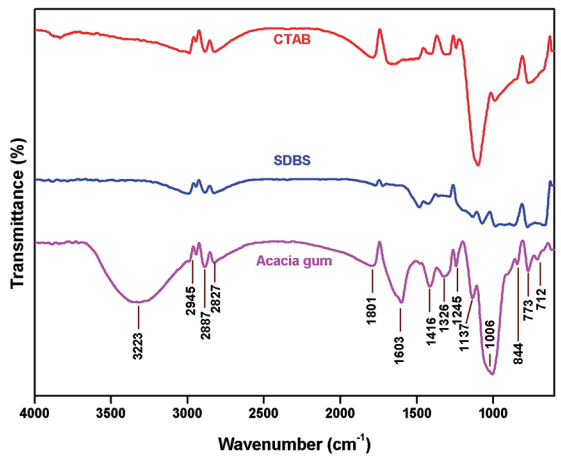

Figure 7: FTIR Spectra of In_2O_3 samples capped with (a) CTAB (b) SDBS

Table 4: FTIR data of In_2O_3 samples capped with CTAB and SDBS

	C-H Vibration	Absorption of C-O Vibration	C-O Vibration from Acetyl-acetonate
CTAB	2990cm^{-1}	1790 cm^{-1}	1665 cm^{-1}
SDBS	2925 cm^{-1}	1723cm^{-1}	1723 cm^{-}

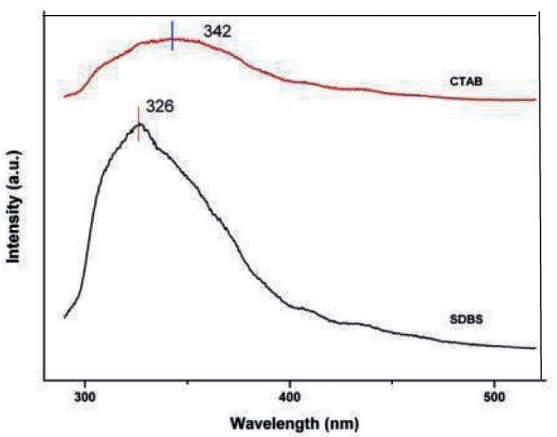

Figure 8: Room temperature PL Spectra of In_2O_3 samples capped with (a) CTAB (b) SDBS calcined at 650°C

SEM and TEM techniques. The average particle size of the nanoparticles determined by TEM and XRD analyses was almost same and was found to be 16nm with CTAB surfactant and 17nm with SDBS surfactant. The particles

were spherical and spherical cluster shaped respectively with no tendency of agglomeration. Raman and UV-Vis spectral analysis confirmed that the band gap value of CTAB capped In_2O_3 particles were larger than the SDBS capped In_2O_3 particles. FTIR analysis indicated that the bands were stretched in In_2O_3 particles capped by SDBS than by CTAB. From the photoluminescence studies (PL technique), a blue shift in the emission peaks of CTAB and SDBS capped In_2O_3 particles was observed, that indicates presence of In_2O_3 NPs.

6. References

1. Qurashi A, El-Maghraby EM, Yamazaki T, Kikuta T. Catalyst-free shape controlled synthesis of In_2O_3 pyramids and octahedron: Structural properties and growth mechanism. *Journal of Alloys and Compounds*. 2009;480(2):L9-L12.

2. Mohanta D, Ahmed GA, Choudhury A, Singh F, Avasthi DK. Properties of 80-MeV oxygen ion irradiated ZnS:Mn nanoparticles and exploitation in nanophotonics. *Journal of Nanoparticle Research*. 2006;8(5):645-652.

3. Qurashi A, Yamazaki T, El-Maghraby EM, Kikuta T. Fabrication and gas sensing properties of In_2O_3 nanopushpins. *Applied Physics Letters*. 2009;95(15):153109.

4. Granqvist CG. Transparent conductive electrodes for electrochromic devices: A review. *Applied Physics A*. 1993;57(1):19-24.

5. Steffes H, Imawan C, Solzbacher F, Obermeier E. Enhancement of NO_2 sensing properties of In_2O_3-based thin films using an Au or Ti surface modification. *Sensors and Actuators B: Chemical*. 2001;78(1-3):106-112.

6. Tanaka S, Esaka T. Characterization of NO_x sensor using doped In_2O_3. *Journal of Materials Research*. 2001;16(5):1389-1395.

7. Hafeezullah, Yamani ZH, Iqbal J, Qurashi A, Hakeem A. Rapid sonochemical synthesis of In_2O_3 nanoparticles their doping optical, electrical and hydrogen gas sensing properties. *Journal of Alloys and Compounds*. 2014;616:76-80.

8. Rumyantseva MN, Ivanov VK, Shaporev SA, Rudyi YM, Yushchenko VV, Arbiol J, et al. Microstructure and sensing properties of nanocrystalline indium oxide prepared using hydrothermal treatment. *Russian Journal of Inorganic Chemistry*. 2009;54(2):163-171.

9. Eranna G, Joshi BC, Runthala DP, Gupta RP. Oxide Materials for Development of Integrated Gas Sensors—A Comprehensive Review. *Critical Reviews in Solid State and Materials Sciences*. 2004;29(3-4):111-188.

10. Epifani M, Siciliano P, Gurlo A, Barsan N, Weimar U. Ambient Pressure Synthesis of Corundum-Type In_2O_3, *Journal of the American Chemical Society*. 2004;126(13):4078-4079.

11. Murali A, Barve A, Leppert VL, Risbud SH, Kennedy IM, Lee HWH. Synthesis and Characterization of Indium Oxide Nanoparticles. *Nano Letters*. 2001;1(6):287-289.

12. Rey JFQ, Plivelic TS, Rocha RA, Tadokoro SK, Torriani I, Muccillo ENS. Synthesis of In_2O_3 nanoparticles by thermal decomposition of a citrate gel precursor. *Journal of Nanoparticle Research*. 2005;7(2):203-208.

13. Bao-Long Y, Hong-Jian B, Xiao-Chun W, Gui-Lan Z, Guo-Qing T, Wen-Ju C, et al. Non-linear optical properties of In_2O_3 nanoparticles. *Acta Physica Sinica*. 1999;48(2):320-325.

14. Zhan ZL, Song W, Jiang D. Preparation of nanometer-sized In_2O_3 particles by a reverse micro emulsion method. *Journal of Colloid and Interface Science*. 2004;271(2):366-371.

15. Joseph Prince J, Ramamurthy S, Subramanian B, Sanjeeviraja C, Jayachan M. Spray pyrolysis growth and material properties of In_2O_3 films. *Journal of Crystal Growth*. 2002;240(1-2):142-151.

16. Yang H, Tang A, Zhang X, Yang W, Qiu G. In_2O_3 nanoparticles synthesized by mechanochemical processing. *Scripta Materialia*. 2004;50(4):413-415.

17. Zhu BL, Xie CS, Zeng DW, Wang AH, Song WL, Zhao XZ. New method of synthesizing In_2O_3 nanoparticles for application in volatile organic compounds (VOCs) gas sensors. *Journal of Materials Science*. 2005;40(21):5783-5785.

18. Niederberger M, Garnweitner G, Buha J, Polleux J, Ba J, Pinna N. Nonaqueous synthesis of metal oxide nanoparticles: Review and indium oxide as case study for the dependence of particle morphology on precursors and solvents. *Journal of Sol-Gel Science and Technology*. 2006;40(2):259-266.

19. Xu J, Wang X, Shen J. Hydrothermal synthesis of In_2O_3 for detecting H_2S in air. *Sensors and Actuators B: Chemical*. 2006;115(2):642-646.

20. Shigesato Y, Takaki S, Haranoh T. Electrical and structural properties of low resistivity tin-doped indium oxide films. *Journal of Applied Physics*. 1992;71(7):3356-3364.

21. Takada T, Suzuki K, Nakane M. Highly sensitive ozone sensor. *Sensors and Actuators B: Chemical*. 1993;13(1-3):404-407.

22. P. Guha, S. Kar, S. Chaudhuri, Direct synthesis of single crystalline In_2O_3 nanopyramids and nanocolumns and their photoluminescence properties. *Applied Physics Letters.* (2004); 85: 3851-3853.

23. Hamburg I, Granqvist CG. Evaporated Sn-doped In_2O_3 films: Basic optical properties and applications to energy-efficient windows. *Journal of Applied Physics*. 1986;60(11):R123-R159.

24. Lei Z, Ma G, Liu M, You W, Yan H, Wu G, et al. Sulfur-substituted and zinc-doped $In(OH)_3$: A new class of catalyst for photocatalytic H_2 production from water under visible light illumination. *Journal of Catalysis*. 2006;237(2):322-329.

25. Li C, Lian S, Liu Y, Liu S, Kang Z. Preparation and photoluminescence study of mesoporous indium hydroxide nanorods. *Materials Research Bulletin*. 2010;45(2):109-112.

26. Nakata A, Mizuhata M, Deki S. Novel fabrication of highly crystallized nanoparticles in the confined system by the liquid phase deposition (LPD) method. *Electrochimica Acta*. 2007;53(1):179-185.

27. Gupta A, Pandya DK, Kashyap SC. Thin fluorine- Doped Tin Oxide Films Prepared Using an Electric Field-Modified Spray Pyrolysis Deposition Technique. *Japanese Journal of Applied Physics*. 2004;43(Pt 2)(12B):L1592-L1594.

28. Leite ER, Gomes JW, Oliveira MM, Lee EJ, Longo E, Varela JA, et al. Synthesis of SnO2 nanoribbons by a carbothermal reduction process. *Journal of Nanoscience and Nanotechnology*. 2002;2(2):125-128.

29. Mryasov ON, Freeman AJ. Electronic band structure of indium tin oxide and criteria for transparent conducting behavior. *Physical Review B*. 2001;64(23):233111.

30. Yang J, Lin C, Wang Z, Lin J. $In(OH)_3$ and In_2O_3 nanorod bundles and spheres: Micro emulsion mediated hydrothermal synthesis and luminescence properties. *Inorganic Chemistry*. 2006;5(22):8973-8979.

31. Seetha M, Bharathi S, Dhayal Raj A, Mangalaraj D, Nataraj D. Optical investigations on indium oxide nano-particles prepared through precipitation method. *Materials Characterization*. 2009;60(12):1578-1582.

32. Wang CY, Dai Y, Pezoldt J, Lu B, Kups T, Cimalla V, et al. Phase stabilization and phonon properties of single crystalline rhombohedral Indium Oxide. *Crystal Growth & Design*. 2008;8(4):1257-1260.